

Received March 26, 2020, accepted March 31, 2020, date of publication April 3, 2020, date of current version April 17, 2020.

Digital Object Identifier 10.1109/ACCESS.2020.2985416

# Automatic Identification of Coronary Arteries in Coronary Computed Tomographic Angiography

CHENG-JUN ZHANG<sup>1,2,3</sup>, DENGHUI XIA<sup>1,2,3</sup>, CHAO ZHENG<sup>2</sup>, JIANYONG WEI<sup>2</sup>, YU CUI<sup>2</sup>, YANZHEN QU<sup>1,3,4</sup>, (Senior Member, IEEE), AND FANGZHOU LIAO<sup>2,5</sup>

<sup>1</sup>School of Computer and Software, Nanjing University of Information Science and Technology, Nanjing 210044, China

<sup>2</sup>Yukun Beijing Network Technology Company Ltd., Beijing 102200, China

<sup>3</sup>Jiangsu Engineering Center of Network Monitoring, Nanjing University of Information Science and Technology, Nanjing 210044, China

<sup>4</sup>School of Computer Science and Technology, Colorado Technical University, Colorado Springs, CO 80907, USA

<sup>5</sup>Institute of Information Engineering, Chinese Academy of Sciences, Beijing 100864, China

Corresponding author: Fangzhou Liao (liaofangzhou@ie.ac.cn)

This work was supported in part by the National Natural Science Foundation of China under Grant 61703212.

**ABSTRACT** Cardiovascular disease has seriously affected the lives of modern people. One of the most commonly used imaging methods for diagnosing cardiovascular disease is computed tomography angiography (CTA). To generate a diagnosis report for doctors, every coronary artery needs to be identified and segmented, including the right coronary artery (RCA), the posterior descending artery (PDA), the posterior lateral branch (PLB), the left circumflex (LCx), the left anterior descending branch (LAD), the ramus intermedius (RI), the obtuse marginal branches (OM1, OM2), and the diagonal branches (D1, D2). In this paper, we proposed a coronary artery automatic identification algorithm, which performs better in terms of accuracy than other similar algorithms and works efficiently. Normally, each Coronary Computed Tomographic Angiography (CCTA) dataset can be completed within seconds. This algorithm fully complies with the coronary label standard established by the Society of Cardiovascular Computed Tomography (SCCT). This algorithm has been put into operation in more than 100 hospitals for over one year. According to all previous tests, the labels obtained from the algorithm were compared with results manually corrected by several experts. Among 892 CCTA datasets, 95.96% of the labels obtained from the algorithms were correct.

**INDEX TERMS** Automatic identification, computed tomography angiography, coronary artery.

## I. INTRODUCTION

Coronary computed tomographic angiography (CCTA) is a non-invasive imaging modality that can visualize the heart as well as the coronary arteries and has become the main method for diagnosing coronary artery disease [1], [2]. It can provide not only anatomical information on coronary arteries but also pathological information such as the presence and extent of calcifications and stenosis, which are useful in the diagnosis and treatment of coronary artery disease [3], [4]. Due to the fact that CCTA datasets are composed of a series of 2D images, doctors have to manually complete the post-processing work on a CT workstation and then, on the basis of the postprocessed images, complete the diagnosis report, which can be quite time-consuming [5]–[9]. The automatic postprocessing and diagnosis of CCTAs can significantly

reduce doctors' workloads as well as the time spent on completing diagnostic reports [10]–[12]. In this sense, a cardiac coronary artery automatic identification algorithm is essential since all this diagnostic work is based on the accurate identification of coronary arteries.

A standard diagnostic report must clearly indicate the labels and locations of the coronary arteries in which a lesion occurred [13], [14]. To generate the automatic diagnostic report efficiently and accurately, the identification of coronary arteries should be in strict accordance with the CCTA standards [14], [15]. According to the CCTA standards, coronary arteries are divided into eighteen segments [12]–[16].

In the past few years, some researchers have studied related issues. Yang, Guanyu, *et al.* designed a two-step method implemented by means of a statistical coronary tree model to identify the optimal labeling result of a coronary artery tree [12]. In the first step, it identifies the four main arteries,

The associate editor coordinating the review of this manuscript and approving it for publication was Kin Fong Lei.

including the RCA, LM, LCx and LAD, and then based on the first step, the method identifies all the side branches. The overall accuracy of the method is approximately 92.94%. Cao, Qing, *et al.* proposed a method that extracts the centerlines from coronary computed tomography angiography (CCTA) images, determining their labels by establishing three-dimensional (3D) models for both right-dominant (RD) and left-dominant (LD) coronary circulations [17]. Wu, Dan, *et al.* proposed a method based on long short-term memory (LSTM). The method establishes a TreeLab-Net combining a multilayer perceptron (MLP) encoder network and a bidirectional tree-structural long short-term memory [18]. The net uses the spatial locations and directions of arteries as features and performs an evaluation by a tenfold cross-validation.

Generally, all these methods enjoy a relatively high accuracy. However, the performances of all these methods are not very stable; they may perform well on the four main arteries, such as the RCA, LAD, LCx and LM, but their accuracy is relatively low on the side branches, such as the Right Posterior Descending Artery (R-PDA), Right Posterior Lateral Branch (R-PLB), D1 and D2. However, the importance of the side branches should not be ignored, as they may represent the only source of blood supply to the myocardium, which has very little redundant blood supply. In clinical practice, it is quite common to find examiners whose side branches (such as large diagonal arteries or large marginal arteries) are responsible for a large proportion of the myocardium blood supply. In addition to this, once these side branches have lesions and stenosis that cause hemodynamic changes, the myocardium that relies on the blood supply from these side branches will inevitably be injured. Moreover, the conduction system of the heart also receives blood from the side branches. Therefore, a lesion on the side branches can not only cause myocardial ischemia and myocardial necrosis but also lead to vascular occlusion and a variety of arrhythmia.

The main advantage of the method proposed in the paper is that it enjoys an overall accuracy of 95.96% and its performance on the four main arteries is almost 100%. At the same time, high accuracy is achieved on the side branches. In addition, this method enjoys a higher efficiency, normally processing each CCTA dataset within seconds.

In this paper, we propose an automatic coronary artery identification algorithm that can automatically output the identification of coronary arteries efficiently. It is fair to say that this algorithm is an important prerequisite for the automatic generation of coronary diagnostic reports. At the same time, the accuracy of the algorithm can be up to 95.96%, which is much higher than that of other CT workstations. This work does not try to identify L-PLB and L-PDA because most diagnosis processes do not consider these two arteries [13], [14].

## II. DATA ANALYSIS AND METHODS

This algorithm has been put into operation in more than 100 hospitals for over one year and has processed the data

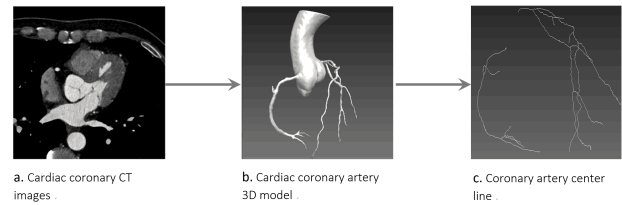


**FIGURE 1.** Extraction of the artery centerlines of a 3D image of a coronary artery.

of thousands of patients. In this research, we collected 892 CCTA datasets from different hospitals. According to the processing pipeline, our research can be divided into several successive steps: centerline extraction, artery branch segmentation and naming. These steps are described in the following paragraphs.

### A. CENTERLINE OF THE CORONARY ARTERY

This algorithm relies on the centerline of the coronary arteries in the heart [19]–[22]. The heart coronary artery centerline can be generated as presented below, and the process is demonstrated in Fig. 1.

- Obtain CT images of the coronary arteries.
- Reconstruct 3D models of the coronary arteries from the CT images.
- Extract the artery centerlines of the 3D coronary artery models.

The centerlines are saved in different VTK-formatted files, which preserve the three-dimensional coordinates of each point of the centerlines [23]–[26]. The  $x$ -axis of the coordinates is the right-to-left shoulder direction of a person, and the direction toward the left shoulder is the positive direction. The  $y$ -axis direction is perpendicular to the chest, and the forebreast is the positive direction of the  $y$ -axis. Downward along the body, the direction that is perpendicular to the  $XY$  plane and pointed toward the feet is the positive direction of the  $z$ -axis. The coronary arteries can be structurally considered as two tree-like structures [27], and Fig. 2 shows the extraction of the original coronary vascular centerline.

## III. RESULTS

### A. DISTINGUISHING BETWEEN THE LEFT CORONARY ARTERY AND RIGHT CORONARY ARTERY

The first step of this method is to distinguish the left coronary artery from the right one. In general, the left coronary artery is on the positive side of the  $x$ -axis, while the right coronary artery is on the negative side of the  $x$ -axis. We designed the following scheme to distinguish the left coronary artery and the right coronary artery: calculate the mean of the  $x$ -coordinates of all points on the left and right coronary arteries; the coronary artery with the larger mean  $x$ -coordinate value is the left coronary artery, and the coronary artery with the smaller mean  $x$ -coordinate value is the right coronary artery.



FIGURE 2. The centerline of a coronary artery.

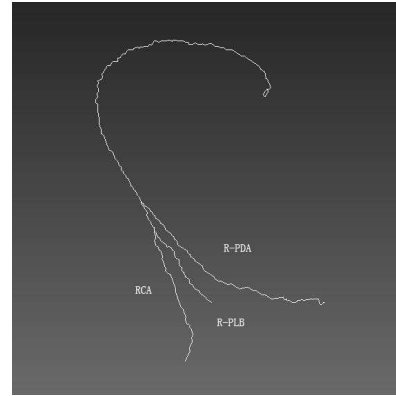


FIGURE 3. The RCA, R-PDA and R-PLB in the right coronary artery.

### B. IDENTIFICATION OF THE RCA, R-PDA AND R-PLB FROM THE RIGHT CORONARY ARTERY

In Fig. 3, we are mainly concerned with three blood arteries, i.e., RCA, R-PDA and R-PLB, in the right coronary section. The RCA is determined on the basis of the following criteria:

- Identify the arteries that are maximal in the direction of the  $y$ -axis and, at the same time, have a relatively high value (higher than at least 0.8 times the maximum of the  $z$ -axis in the right coronary) in the  $z$ -axis direction; denote these blood arteries as possible RCAs.
- Compare the  $y$ -axis coordinates of the endpoint of the possible RCAs with the  $y$ -axis coordinates of the original point of the right coronary artery. If the  $Y$  coordinate of a possible RCA end point is larger, then this RCA is the RCA; otherwise, go to the next step.
- Find an artery with the maximum value in the  $z$ -axis direction; define it as the RCA.

At the beginning of the RCA, the artery tends to descend gently along the negative direction of the  $x$ -axis, which can be defined as the Proximal Right Coronary Artery (pRCA); then, it moves quickly along the positive direction of the  $z$ -axis, which can be defined as the Mid right coronary artery (mRCA). When it descends to the bottom of the heart, it slowly extends along the positive direction of the  $x$ -axis and  $y$ -axis, which can be defined as the Distal Right Coronary Artery (dRCA).

The method of identifying the R-PLB and R-PDA is as follows:

- Determine the starting point of the left coronary artery as the left root and the starting point of the right coronary artery as the right root. Calculate their midpoint coordinates “midRoot [ $x, y, z$ ]”.
- At the bottom of the RCA, find all branch arteries that point to the positive  $x$ -axis direction or negative  $y$ -axis direction. According to the order of appearance of these blood arteries on the RCA, these blood arteries are sequentially stored in an array “PDA\_PLB\_possible\_list”.
- On the X-Y plane, calculate the distance between all blood arteries in PDA\_PLB\_possible\_list and the “mid-point”. The blood artery in PDA\_PLB\_possible\_list

with the smallest distance is the R-PLB. If PDA\_PLB\_possible\_list is empty, the R-PDA and R-PLB do not exist.

- Of all the arteries in PDA\_PLB\_possible\_list, the longest one after the R-PDA is the R-PLB. If there are no blood arteries after the R-PDA, then the R-PLB does not exist.

### C. IDENTIFICATION OF THE pRCA, mRCA AND dRCA

The identification process is shown in Fig. 4. The cutting point of the pRCA and mRCA can be detected as follows: define  $n = 20$  and  $i = 0$ , choose the  $i^{\text{th}}$  point of the pRCA,  $RCA[i]$ , and the  $n^{\text{th}}$  point,  $RCA[i + n]$ , and then calculate  $tg(RCA[i], RCA[i + n])$  according to formula 1.

$$tg(P_1, P_2) = \frac{|z_1 - z_2|}{MAX(|x_1 - x_2|, |y_1 - y_2|)} \quad (1)$$

If  $tg(RCA[i], RCA[i + n]) \geq 1$ , then point  $RCA[(i+n)/2]$  is the cutting point of the pRCA and mRCA; otherwise,  $i = i + 1$  until  $i$  reaches the middle point of the RCA. The method for detecting the cutting point of the mRCA and dRCA is similar to the mentioned method.

### D. IDENTIFICATION OF THE LM, LCx AND LAD FROM THE LEFT CORONARY ARTERY

Fig. 5 shows the identification of these left-side blood arteries. The LCx extends in the positive direction of the  $y$ -axis or the negative direction of the  $x$ -axis, and the LAD extends in the negative direction of the  $y$ -axis or the positive direction of the  $x$ -axis. Therefore, theoretically, the overlapping part of the LAD and LCx is defined as the LM.

Following the steps below, one can accurately identify the LM, LAD, and LCx in more than 60% of the cases:

- Find the common part of all left coronary arteries and name it the LM.
- In all bifurcation arteries after the LM, find a blood artery that extends along the positive direction of the  $y$ -axis or the negative direction of the  $x$ -axis, which can achieve the maximum in the  $z$ -axis direction, and define it as the LCx. Find a blood artery that extends

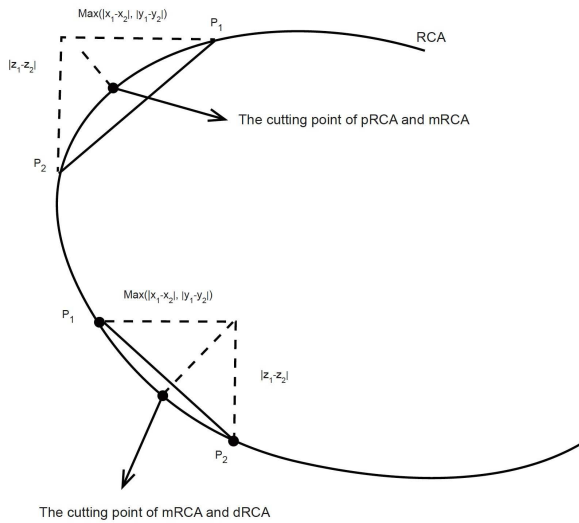


**FIGURE 4.** Identification of the cutting point for the pRCA, mRCA and dRCA.

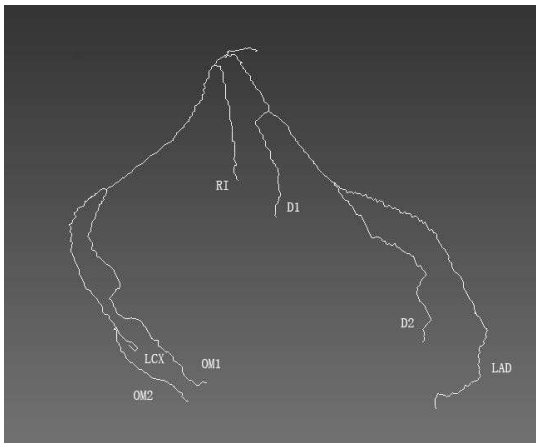


**FIGURE 5.** The LAD, LCx, OM1, OM2, D1, D2, OM1, OM2, and RI in the left coronary artery.

along the positive direction of the  $x$ -axis or the negative direction of the  $y$ -axis, which can achieve the maximum in the  $z$ -axis direction, and define it as the LAD.

However, due to variations in the coronary blood arteries, there are often branches and burrs of varying length on the LM, which can easily be mistaken as the LAD and LCx. As shown in Fig. 6, there is one burr artery on the LM, which can be mistakenly recognized as an LAD. In practice, this type of burr blood artery may occur more often and vary in length. To solve this problem, we propose the following solution.

- First, it is clear that the Left main Coronary Artery (LM) is the overlapped part of the LAD and LCx. At the same time, the length of the LM is limited, and the maximum length is no more than  $LMMax = 2$  cm.
- Find all combinations of suspected LADs and LCxs based on the previously defined characteristics of the LAD and LCx.



**FIGURE 6.** The burr blood arteries on the LM, which can be mistakenly recognized as LADs.

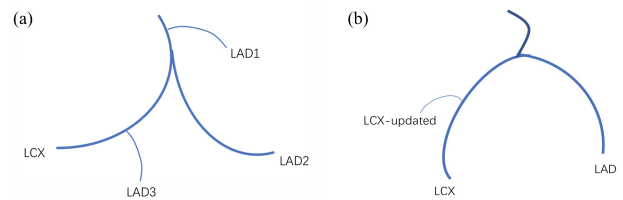


**FIGURE 7.** Identification of LCx and LAD. (a) Different combinations of LAD and LCx. (b) Adjustment of LCx to LCx<sub>updated</sub>.

- For each set of LAD and LCx combinations, obtain the LM and  $abs(\text{length(LAD)} - \text{length(LCx)})$  for this set of LADs and LCxs.
- Find the combination of LADs and LCxs with the smallest  $abs(\text{length(LAD)} - \text{length(LCx)})$  and, at the same time, ensure that  $\text{length(LM)} < LMMax$ ; then, this LAD and LCx pair can be defined as the real LAD and LCx.

As we can see in Fig. 7a, there are three combinations of LADs and LCxs: (LCx, LAD1), (LCx, LAD2) and (LCx, LAD3). For (LCx, LAD3), the length of the LM in this case is too large; thus, this combination is ruled out. For the remaining two combinations (LCx, LAD1) and (LCx, LAD2),  $abs(\text{length(LAD2)} - \text{length(LCx)}) < abs(\text{length(LAD1)} - \text{length(LCx)})$ . Therefore, LCx and LAD2 are the real LCx and LAD. On the LCx identified in the last step, determine whether there are blood arteries that are on the LCx and pointing toward the outside of the angle between the LAD and LCx. If there are such blood arteries, then the first existing one can be defined as the real LCx. The adjustment of the LCx is shown in Fig. 7b, where the LCx is adjusted to LCx<sub>updated</sub>.

### E. IDENTIFICATION OF OM1 AND OM2 ON THE LCx

The blood arteries on the LCx pointing toward the inside of the angle between the LAD and LCx are called OM1 and OM2, and those on the LAD pointing toward the inside of the angle between the LAD and LCx are called D1 and D2. OM1,

OM2, D1, and D2 may not exist. The process of identifying OM arteries is as follows:

- Find all the branches from the LCx, and put them into “OM1OM2List”.
- In the order of their appearance on the LCx, find 3 blood arteries in “OM1OM2List” pointing toward the inside of the angle between the LAD and LCx. These are OM1, OM2 and OM3.
- The basis for judging whether the branch is an OM is whether this blood artery points toward the inside of the angle between the LCx and LAD.
- Since the LAD is in the positive direction of the LCx and because the LAD and LCx are close together along the y-axis, the definition of an OM blood artery is as follows: relative to the LCx, the blood arteries that are oriented in the positive direction along the X-axis are OMs.

It is important to realize that Proximal Left Circumflex (pCx) is defined from the end of the LM to the start of OM1; after pCx, the remaining portion of the Mid and distal Left Circumflex (LCx) is called the LCx.

#### F. IDENTIFICATION OF D1, D2, AND D3 ON THE LAD

The process of identifying D1, D2 and D3 is as follows:

- Find all the branch arteries from the LAD, and put them into “Dlist”.
- In the order of their appearance on the LAD, find three blood arteries in “Dlist” pointing toward the positive direction of the y-axis; these are the *D* arteries.

Since D1 and D2 are identified, the Proximal Left Anterior Descending Branch (pLAD), Mid Left Anterior Descending Branch (mLAD) and Distal Left Anterior Descending Branch (dLAD) are regarded as 3 divisions of the LAD, where the cutting points are the starting points of the OM branches. Since OM1 and OM2 are already identified, the pLAD, mLAD and dLAD can be easily identified.

#### G. IDENTIFICATION OF THE RI

The RI is defined as a blood artery sandwiched between the LAD and LCx. The rule for identifying the RI is as follows: if the distance between the last point of the LM and the starting point of OM1 or D1 is less than 6 points, then OM1 or D1 should be renamed the RI. In this case, OM2 and OM3 (if they exist) should be renamed OM1 and OM2, respectively; similarly, D2 and D3 (if they exist) should be renamed D1 and D2, respectively.

The whole automatic identification algorithm was completed in Python2.0 with an 8 GB 1867 MHz DDR3 processor in the macOS system, and our method has a competitive computational time of less than half a minute on average for one case. All cases acquired by the GE revolution scanner are used to evaluate the algorithm in this framework. In each case, 16 segments are named based on the centerline. After the process is completed, experts review the results according to the SCCT label standard and judge whether or not they are accurate. The correct criterion for the algorithm is that all

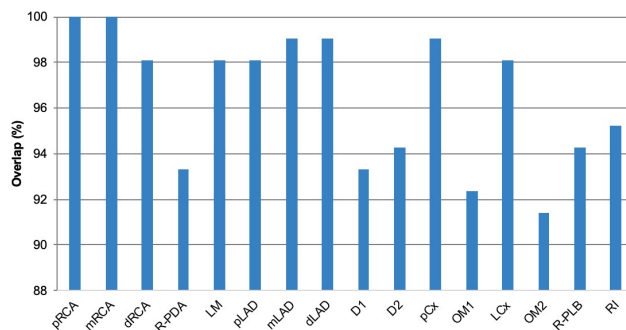


FIGURE 8. The average overlap between the automatic identification and the correct results for 16 levels on all datasets.

segments are correctly named. The evaluation results show that the accuracy of the algorithm can reach 95.96%.

#### IV. CLINICAL EVALUATION

To test the effectiveness and the accuracy of the algorithm, the algorithm was evaluated by four experts at Beijing Friendship Hospital on datasets including 892 clinical cases that contained various artery pathologies and image qualities. These datasets were from patients who had sequentially undergone CCTA imaging. All the arteries and their centerlines in each dataset were detected successfully. The performance of the algorithm was measured by two metrics: the overall overlap (OOV) and the average overlap (AOV). For the OOV, only if all 16 segments are correctly named can the result be labeled as correct. The results for OOV is about 78%, meaning that most results can be directly used without any correction. The AOV measures the accuracy in the identification of every single blood artery. The details of the AOV are displayed in Fig. 8 and the accuracy of OOV is up to 95.96%.

#### V. DISCUSSION AND ALGORITHM VALIDATION

In this paper, we proposed a rule-based algorithm that can segment and identify coronary arteries according to the SCCT standard. The L-PLB and L-PDA were not included in the manual correction since they have no clinical relevance. For now, this algorithm has met the requirements of a coronary heart disease automatic diagnosis system and has showed important clinical significance for improving diagnostic efficiency. Actually, this coronary heart disease automatic diagnosis system has been deployed to several hospitals in China and is highly appreciated by doctors.

In our design, we plan to carry out automatic validation for each processing outcome. The validation phase will be developed by using a deep learning model that will check for various “variant cases”: for example, the RCA may be extremely short or may point backward toward the heart, or the LCx may be very short, while the OM1 and OM2 are very long. Hence, the accuracy of the entire processing will be further improved.

In this work, we presented a fully automatic identification algorithm for coronary arteries in CCTA images based on

the SCCT standard. A quantitative clinical evaluation showed that our method was able to name coronary arteries with high overlap and high accuracy. This algorithm will greatly benefit research work and clinical practice regarding, for example, automated report generation.

## COMPETING INTERESTS

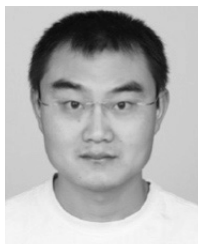
There are no competing interests in this study.

## LIST OF ABBREVIATIONS

Society of Cardiovascular Computed Tomography (SCCT); Coronary Computed Tomographic Angiography (CCTA); Proximal Right Coronary Artery (pRCA); Mid-Right Coronary Artery (mRCA); Distal Right Coronary Artery (dRCA); Right Posterior Descending Artery (R-PDA); Left Main Coronary Artery (LM); Proximal Left Anterior Descending Branch (pLAD); Mid Left Anterior Descending Branch (mLAD); Distal Left Anterior Descending Branch (dLAD); First Diagonal Branch (D1); Second Diagonal Branch (D2); Proximal Left Circumflex (pCx); Mid and distal Left Circumflex (LCx); First Obtuse Marginal Branch (OM1); Second Obtuse Marginal Branch (OM2); Left Posterior Descending Artery (L-PDA); Ramus Intermedius (RI); Right Posterior Lateral Branch (R-PLB); Left Posterior Lateral Branch (L-PLB).

## REFERENCES

- [1] F. Bamberg, A. Becker, F. Schwarz, R. P. Marcus, M. Greif, F. von Ziegler, R. Blankstein, U. Hoffmann, W. H. Sommer, V. S. Hoffmann, T. R. C. Johnson, H.-C.-R. Becker, B. J. Wintersperger, M. F. Reiser, and K. Nikolaou, "Detection of hemodynamically significant coronary artery stenosis: Incremental diagnostic value of dynamic CT-based myocardial perfusion imaging," *Radiology*, vol. 260, no. 3, pp. 689–698, Sep. 2011.
- [2] Z. Cheng, X. Wang, Y. Duan, L. Wu, D. Wu, C. Liang, C. Liu, and Z. Xu, "Detection of coronary artery anomalies by dual-source CT coronary angiography," *Clin. Radiol.*, vol. 65, no. 10, pp. 815–822, Oct. 2010.
- [3] W. G. Hundley, D. A. Bluemke, J. P. Finn, S. D. Flamm, M. A. Fogel, M. G. Friedrich, V. B. Ho, M. Jerosch-Herold, C. M. Kramer, W. J. Manning, M. Patel, G. M. Pohost, A. E. Stillman, R. D. White, and P. K. Woodard, "ACCF/ACR/AHA/NASCI/SCMR 2010 expert consensus document on cardiovascular magnetic resonance: A report of the American college of cardiology foundation task force on expert consensus documents," *J. Amer. College Cardiol.*, vol. 55, pp. 2614–2662, Jun. 2010.
- [4] G. Mowatt, J. A. Cook, G. S. Hillis, S. Walker, C. Fraser, X. Jia, and N. Waugh, "64-slice computed tomography angiography in the diagnosis and assessment of coronary artery disease: Systematic review and meta-analysis," *Heart*, vol. 94, no. 11, pp. 1386–1393, Nov. 2008.
- [5] P. Angelini, J. A. Velasco, and S. Flamm, "Coronary anomalies: Incidence, pathophysiology, and clinical relevance," *Circulation*, vol. 105, no. 20, pp. 2449–2454, May 2002.
- [6] M. Dirksen, J. Bax, N. Blom, M. Schalij, W. Jukema, H. Vliegen, E. van der Wall, A. de Roos, and H. Lamb, "Detection of malignant right coronary artery anomaly by multi-slice CT coronary angiography," *Eur. Radiol.*, vol. 12, no. S3, pp. S177–S180, Dec. 2002.
- [7] Y. Wang and P. Liatsis, "Automatic segmentation of coronary arteries in CT imaging in the presence of kissing vessel artifacts," *IEEE Trans. Inf. Technol. Biomed.*, vol. 16, no. 4, pp. 782–788, Jul. 2012.
- [8] A. Khedmati, A. Nikravanshalmani, and A. Salajegheh, "Semi-automatic detection of coronary artery stenosis in 3D CTA," *IET Image Process.*, vol. 10, no. 10, pp. 724–732, Oct. 2016.
- [9] D. Lesage, E. D. Angelini, I. Bloch, and G. Funka-Lea, "A review of 3D vessel lumen segmentation techniques: Models, features and extraction schemes," *Med. Image Anal.*, vol. 13, no. 6, pp. 819–845, Dec. 2009.
- [10] F. Cademartiri, L. La Grutta, R. Malagò, F. Alberghina, W. B. Meijboom, F. Pugliese, E. Maffei, A. A. Palumbo, A. Aldrovandi, M. Fusaro, V. Brambilla, P. Coruzzi, M. Midiri, N. R. A. Mollet, and G. P. Krestin, "Prevalence of anatomical variants and coronary anomalies in 543 consecutive patients studied with 64-slice CT coronary angiography," *Eur. Radiol.*, vol. 18, no. 4, pp. 781–791, Apr. 2008.
- [11] F. Cademartiri, G. Runza, G. Luccichenti, M. Galia, N. R. Mollet, V. Alaimo, V. Brambilla, M. Gualerzi, P. Coruzzi, M. Midiri, and R. Lagalla, "Coronary artery anomalies: Incidence, pathophysiology, clinical relevance and role of diagnostic imaging," *La Radiologia Medica*, vol. 111, no. 3, pp. 376–391, Apr. 2006.
- [12] G. Yang, A. Broersen, R. Petr, P. Kitslaar, M. A. D. Graaf, J. J. Bax, J. H. C. Reiber, and J. Dijkstra, "Automatic coronary artery tree labeling in coronary computed tomographic angiography datasets," *Comput. Cardiol.*, pp. 109–112, Mar. 2012.
- [13] W. Austen, J. Edwards, R. Frye, G. Gensini, V. Gott, L. Griffith, D. McGoon, M. Murphy, and B. Roe, "A reporting system on patients evaluated for coronary artery disease. Report of the ad hoc committee for grading of coronary artery disease, council on cardiovascular surgery, American heart association," *Circulation*, vol. 51, no. 4, pp. 5–40, Apr. 1975.
- [14] F.-Z. Wu and M.-T. Wu, "2014 SCCT guidelines for the interpretation and reporting of coronary CT angiography: A report of the society of cardiovascular computed tomography guidelines committee," *J. Cardiovascular Comput. Tomogr.*, vol. 9, no. 2, p. e3, Mar./Apr. 2015.
- [15] J. Leipsic, S. Abbara, S. Achenbach, R. Cury, J. P. Earls, G. J. Mancini, K. Nieman, G. Pontone, and G. L. Raff, "SCCT guidelines for the interpretation and reporting of coronary CT angiography: A report of the society of cardiovascular computed tomography guidelines committee," *J. Cardiovascular Comput. Tomogr.*, vol. 8, no. 5, pp. 342–358, Sep. 2014.
- [16] D. Han, H. Shim, B. Jeon, Y. Jang, Y. Hong, S. Jung, S. Ha, and H.-J. Chang, "Automatic coronary artery segmentation using active search for branches and seemingly disconnected vessel segments from coronary CT angiography," *PLoS ONE*, vol. 11, no. 8, 2016, Art. no. e0156837.
- [17] Q. Cao, A. Broersen, M. A. de Graaf, P. H. Kitslaar, G. Yang, A. J. Scholte, B. P. F. Lelieveldt, J. H. C. Reiber, and J. Dijkstra, "Automatic identification of coronary tree anatomy in coronary computed tomography angiography," *Int. J. Cardiovascular Imag.*, vol. 33, no. 11, pp. 1809–1819, Nov. 2017.
- [18] D. Wu, X. Wang, J. Bai, X. Xu, B. Quyan, Y. Li, H. Zhang, Q. Song, K. Cao, and Y. Yin, "Automated anatomical labeling of coronary arteries via bidirectional tree LSTMs," *Int. J. Comput. Assist. Radiol. Surg.*, vol. 14, no. 2, pp. 271–280, Feb. 2019.
- [19] G. Yang, P. Kitslaar, M. Frenay, A. Broersen, M. J. Boogers, J. J. Bax, J. H. C. Reiber, and J. Dijkstra, "Automatic centerline extraction of coronary arteries in coronary computed tomographic angiography," *Int. J. Cardiovascular Imag.*, vol. 28, no. 4, pp. 921–933, Apr. 2012.
- [20] C. T. Metz, M. Schaap, A. C. Weustink, N. R. Mollet, T. van Walsum, and W. J. Niessen, "Coronary centerline extraction from CT coronary angiography images using a minimum cost path approach," *Med. Phys.*, vol. 36, no. 12, pp. 5568–5579, Nov. 2009.
- [21] D. A. B. Oliveira, L. Leal-Taixé, R. Q. Feitosa, and B. Rosenhahn, "Automatic tracking of vessel-like structures from a single starting point," *Comput. Med. Imag. Graph.*, vol. 47, pp. 1–15, Jan. 2016.
- [22] L. D. Cohen and T. Deschamps, "Segmentation of 3D tubular objects with adaptive front propagation and minimal tree extraction for 3D medical imaging," *Comput. Methods Biomech. Biomed. Eng.*, vol. 10, no. 4, pp. 289–305, Aug. 2007.
- [23] S. R. Aylward and E. Bullitt, "Initialization, noise, singularities, and scale in height ridge traversal for tubular object centerline extraction," *IEEE Trans. Med. Imag.*, vol. 21, no. 2, pp. 61–75, Feb. 2002.
- [24] R. Tarjan, "Depth-first search and linear graph algorithms," in *Proc. Symp. Switching Automat. Theory*, Jul. 2008, pp. 114–121.
- [25] N. D. Cornea, D. Silver, X. Yuan, and R. Balasubramanian, "Computing hierarchical curve-skeletons of 3D objects," *Vis. Comput.*, vol. 21, no. 11, pp. 945–955, Oct. 2005.
- [26] Y.-S. Wang and T.-Y. Lee, "Curve-skeleton extraction using iterative least squares optimization," *IEEE Trans. Vis. Comput. Graphics*, vol. 14, no. 4, pp. 926–936, Jul./Aug. 2008.
- [27] Q. Cao, A. Broersen, P. H. Kitslaar, B. P. F. Lelieveldt, and J. Dijkstra, "A quality score for coronary artery tree extraction results," *Proc. SPIE*, vol. 10575, Feb. 2018, Art. no. 105750V, doi: 10.1117/12.2292430.



**CHENG-JUN ZHANG** was born in Lu'an, Anhui, China, in 1982. He received the B.S. degree from Jilin University, China, in 2006, the master's degree from the University of Science and Technology of China, in 2010, and the Ph.D. degree in physics from the University of Fribourg, Switzerland, in 2013.

He was a Lecturer with the School of Computer and Software, Nanjing University of Information Science and Technology. Since 2017, he has been a Data Scientist with Yukun Beijing Network Technology Company Ltd., where he began to focus on the application of data mining in medical field. His research interests include complex networks, link prediction, recommender systems, data mining, and deep learning.



**DENGHUI XIA** received the bachelor's degree in network engineering from the Yancheng Institute of Technology, in 2019. He is currently pursuing the master's degree in software engineering with the Nanjing University of Information Science and Technology.

His research interests include complex networks, link prediction, recommendation systems, data mining, and deep learning.



**CHAO ZHENG** received the master's degree in software engineering from the University of Science and Technology of China, in 2009. He was the Chief Architect of the Cloud Fabric Team and the Platform Services, IBM, China, in September 2017. He is the World's First Practitioner to apply deep learning to large-scale commercial distributed cloud platforms. He is also the Core Contributor of the Global PaaS Open Standard. He is currently a CTO with Yukun Beijing Network Technology Company Ltd., Beijing.

His current research interests include cloud computing, artificial neural networks, and machine learning in biomedical image. He received lots of awards, including the Outstanding Technical Achievement Award and the IBM Innovation Technology Award, during his IBM career.



**JIANYONG WEI** was born in Hechi, Guangxi, China, in 1994. She received the bachelor's and master's degrees in biomedical engineering from the Beijing Institute of Technology, Beijing, China, in 2016 and 2018, respectively. During her graduate study, she involved in research projects regarding hemodynamic simulation and computer-aided designs of aortic fast virtual stenting, which were funded by the National Natural Science Foundation of China and the Ministry of Science and Technology.

She is currently a Research Associate with Yukun Beijing Network Technology Company Ltd., Beijing, and devotes to investigate the application of artificial intelligence in cardiovascular and cerebrovascular diseases diagnosis. Her research has published in several international renowned journals such as *Theranostics*.



**YU CUI** received the B.S. and master's degrees from the Beijing University of Posts and Telecommunications, China, in 2010.

He was a Product Designer with Schneider Electric. In 2016, he was with Alibaba Robotics Network Technology Company Ltd., subsidiary of the Alibaba Group. He worked as a Product Manager, and his working focus on the Research and Development and AI Products, such as robots. Since 2017, he has been a Product Director with Yukun Beijing Network Technology Company Ltd., during which he began to focus on the product Research and Development in medical field.



**YANZHEN QU** (Senior Member, IEEE) received the B.Eng. degree in electronic engineering from Anhui University, China, in 1982, the M.Eng. degree in electrical engineering from the Chinese Science Academy, China, in 1984, and the Ph.D. degree in computer science from Concordia University, Canada, in 1991.

Over his Industrial Professional Career, he has served with the various executive level management positions of the Product Research and Development and the Information Technology Operation at several multinational corporations. He has led his multinational engineering teams successfully developed the world first very large real-time commercial systems and technologies. He joined Colorado Technical University, in 2008. From 2012 to 2014, he has led his student teams participated in the yearly U.S. National Security Innovation Competition. Three years in a roll, his student teams have won the finalist among often over 100s of entrants. In 2013, his student team also received the first place. He is currently the Dean and a Professor of computer science and technology with Colorado Technical University, Colorado Springs, CO, USA. He is also the dissertation supervisor of many computer science doctoral students. He and his Doctoral students have published several dozen scholarly articles, some of them received the best paper award at the several IEEE International Conferences. His current research interests include data science, cybersecurity, the Internet of Things, machine learning, e-learning technologies, software engineering, cloud computing, and affective computing.

He has served as the general or the program chair or a keynote speaker at many IEEE, ACM, ASIS, IFIP international conferences or workshops. He is also an editorial board member of several professional peer-reviewed *Computer Science* or *Information Technology* journals. He has been invited as a visiting professor of over 30 international universities.



**FANGZHOU LIAO** received the B.E. degree in chemical biology and the Ph.D. degree in biomedical engineering from Tsinghua University, Beijing, China, in 2013 and 2018, respectively. He holds a postdoctoral position with the Institute of Information Engineering, CAS, and a Research Scientist with Yukun Beijing Network Technology Company Ltd., Beijing. His current research interests include computational neuroscience, artificial neural networks, and machine learning in biomedical image.

...